Influenza Virus Hemagglutinin-induced Cell-Planar Bilayer Fusion: Quantitative Dissection of Fusion Pore Kinetics Into Stages

GRIGORY B. MELIKYAN, WALTER D. NILES, and FREDRIC S. COHEN

From the Department of Physiology, Rush Medical College, Chicago, Illinois 60612

ABSTRACT Cells expressing the influenza virus hemagglutinin (HA) fuse to planar bilayer membranes under acidic conditions. After an electrically quiescent prefusion stage (Q), a fusion pore forms that enlarges in three subsequent stages. A repetitively flickering pore stage (R) develops into a securely open stage (S) that exhibits conductances ranging from a few to tens of nS. The pore then expands to a terminal stage (T) with a large conductance on the order of one microSiemens. We have studied how virus strain, HA receptors in the target bilayer membrane, and cytoskeleton affect the time a fusion pore remains in each stage. These intervals are referred to as waiting times. In the quiescent stage, waiting times were very sensitive to the virus strain and presence of gangliosides (HA receptors) in the bilayer. When bilayers contained gangliosides, the waiting times in the Q stage for cells infected with the PR/8/34 strain of virus were exponentially distributed, whereas waiting times for cells infected with the Japan/305/57 strain were not so distributed. Without gangliosides, the waiting time distribution for PR/8/34 infected cells was complex. The waiting times in the R and S stages of pore growth were exponentially distributed under all tested conditions. Within the R stage, we analyzed the kinetics of the flickering pore by fitting the open and closed time distributions with a sum of two exponentials. Neither the open and closed time distributions nor the flickering pore conductance distributions were appreciably affected by virus strain or gangliosides. Colchicine and cytochalasin B increased the flicker rates, without affecting the waiting time in the R stage. We conclude that variations in amino acid sequences of the HAs and the presence of gangliosides as receptors within the target membrane critically affect the kinetics of fusion pore formation, but do not affect subsequent stages.

INTRODUCTION

Biological membrane fusion is a protein-mediated event (White, 1992). The best characterized fusion protein is the influenza virus hemagglutinin (HA) glycoprotein

(Wiley and Skehel, 1987; Stegmann, Nir, and Wilschut, 1989), an integral membrane protein responsible for both binding and fusion of the viral envelope to the target membrane (White, Kielian, and Helenius, 1983; White, 1992). Because HA can be reconstituted in lipid vesicles (Stegmann, Morselt, Booy, van Breemen, Scherphof, and Wilschut, 1987b), expressed on cell surfaces (Gething and Sambrook, 1982; White, Helenius, and Gething, 1982), and its ectodomain purified, it has been used in a wide range of biochemical and functional studies (Doms, Helenius and White, 1985; Doms and Helenius, 1986; Skehel, Bayley, Brown, Martin, Waterfield, and White, 1982; Stegmann, Hoekstra, Scherpof, and Wilschut, 1986; Harter, James, Bachi, Semenza, and Brunner, 1989; Sarkar, Morris, Eidelman, Zimmerberg, and Blumenthal, 1989). Under mildly acidic conditions, normally found in endosomes, the HA proceeds through multiple intermediate conformations (Puri, Booy, Doms, White, and Blumenthal, 1990; Stegmann, Booy, and Wilschut, 1987a; Stegman, White, and Helenius, 1990). These multiple stages are thought to be the basis for the relatively slow kinetics of HA-mediated fusion, and the pronounced lag time between acidification and fusion as detected biochemically (Blumenthal, Schoch, Puri, and Clague, 1991; Clague, Schoch, and Blumenthal, 1991; Stegmann, Delfino, Richards, and Helenius, 1991) and electrophysiologically (Spruce, Iwata, White, and Almers, 1989; Spruce, Iwata, and Almers, 1991). When two membranes fuse, their separated aqueous spaces become continuous through the connecting fusion pore. A molecular description of fusion requires that the intermediates leading to fusion and the properties of the nascent pore be characterized. The electrical conductances of pores can be detected by time-resolved admittance measurements (Zimmerberg, Curran, Cohen and Brodwick, 1987). When HA-expressing cells are fused to erythrocytes, the small fusion pores for HA-mediated fusion (Spruce et al., 1989, 1991; Zimmerberg, Blumenthal, Sarkar, Curran, and Morris, 1993) show conductances similar to those observed in exocytosis in mast cells (Zimmerberg et al., 1987; Breckenridge and Almers, 1987; Alvarez de Toledo and Fernandez, 1988; Spruce, Breckenridge, Lee, and Almers, 1990; Monck et al., 1990; Curran, Cohen, Chandler, Munson, and Zimmerberg, 1993). In the companion paper (Melikyan, Niles, Peeples, and Cohen, 1993) we demonstrated that pores connecting HA-expressing cells to planar lipid membranes are similar to those of exocytosis and HA-induced cell-cell fusion. Thus, fusion pores can be studied in a system where the target membrane can be manipulated. Here we quantitatively analyze how different virus strains (with altered details of HA structure), gangliosides (known receptors for HA), and the cytoskeleton of infected cells control the kinetics of pore formation and the consequent dynamics of these pores.

MATERIALS AND METHODS

General Procedures

Cell culturing, virus propagation, cell infection, planar bilayer formation, electrical measurements, and data processing have been described (Melikyan et al., 1993). In brief, MDCK cells infected with influenza virus were settled onto voltage clamped horizontal planar bilayers bathed by a pH 6.3 solution at 37°C. 4 min after 15–30 cells established contact with the bilayer, the *cis* solution was acidified to pH 4.9. Fusion was monitored from the currents

in-phase, ΔY_0, and out-of-phase, ΔY_{90}, with an applied sinusoidal voltage. The direct current conductance, ΔY_{dc}, was also obtained. When required, influenza virus infected cells were made permeable by incubating with 40 μg/ml saponin (from Gypsophila, Sigma Chemical Co., St. Louis, MO) in PBS for 15–20 min at room temperature. These cells were washed with PBS and stored on ice. 80–85% of the cells became permeable, as assessed by incubating them with 100 μM ethidium bromide for 1 min and counting the percentage of bright fluorescent cells (Melikyan et al., 1993). Higher concentrations of saponin tended to cause cell lysis. Overall electrical settings and calibrations were verified by incorporating VDAC (mitochondrial outer membrane channels) in planar membranes and checking that $\Delta Y_0 = \Delta Y_{dc}$ and $\Delta Y_{90} = 0$. 2–5 μl of 10 μg/ml VDAC in 1% Triton X-100 was injected into the *cis*-compartment and single channels with conductances of 0.9–1 nS (Colombini, 1989) were observed. Holding potentials in the range of ±30 mV were superimposed on a 10 mV p–p sinewave of frequency 803 Hz. Y_{dc} was measured at positive and negative potentials to account for any errors caused by uncorrected potential shifts, such as small potential differences between electrodes.

Defining Each Stage

Lowering the pH marked the beginning of an electrically quiescent prefusion stage, Q. Fusion, as monitored by admittance changes, was typically initiated with a small pore that repetitively flickered open and closed. We refer to this as the R stage. The pore then irreversibly and securely opened, exhibiting variable conductance behavior in this S stage. The terminal T stage began with a rapid increase in conductance as the pore fully opened to its final large conductance, 400–500 nS for infected MDCK cells (Fig. 1).

Fitting Distributions

In each stage we defined the waiting time as the time between the beginning and end of that stage. We studied the kinetics of the fusion pore from distributions of the waiting times of each stage, denoted t_Q, t_R, and t_S. The moment of transition between Q and R, seen as the onset of pore flickering, and that between S and T, identified by the initiation of the fast final expansion, are well defined (Fig. 1). The transition between R and S, however, is sometimes ambiguous: if Y_{dc} increases for reasons not related to the fusion pore (e.g., nonspecific increases in membrane conductance), the flickering could be obscured by the large Y_{dc} (and therefore large Y_0) changes and the pore misassigned as having entered S. We assigned the moment of the transition to that time when ΔY_0 no longer returned to baseline. This criterion was chosen because it would be strictly correct if changes in ΔY_0 were due only to fusion pores, it was straightforward to apply, and it was not subjective. As a consequence of this criterion, when Y_0 increased without clear pore flickering and ΔY_{90} changes characteristic of fusion were observed, we set $t_R = 0$, treating these pores as a direct $Q \rightarrow S$ transition. If $\Delta Y_{dc} = 0$, this would be a correct assignment. But if $\Delta Y_{dc} \neq 0$, flickering could have been missed. Thus, the flickering R stage could occur for greater than our estimated 70–80% of the pores (Melikyan et al., 1993).

For all stages, waiting time distributions were plotted only for the first cell fusing to each planar membrane. Because the conductances of the pores of later fusing cells were obscured by prior large admittance increases, their waiting times could not be measured. Fusions of cells to the planar membrane were well separated in time, as determined from ΔY_{90} jumps and fluorescence increases due to ethidium bromide entering the cell through fusion pores (Melikyan et al., 1993). This temporal separation allowed counting the total number of fused cells that reached the T stage. This separation of events is in accord with the measured low efficiency of fusion. Therefore, we assumed that pores of subsequent fusing cells did not form until the first pore entered the T stage.

We defined $P(t)$ as the probability that a cell that will eventually fuse has not yet fused at time

t. The distributions of $P(t)$ therefore present the probability that an event occurred at time $> t$ vs t. Thus, the waiting time distributions monotonically decay from $P(0) = 1$. When the distributions exhibited an appreciable lag, they were fit with two exponentials according to a three-state (two-transition) chain formalism. These distributions were described by $P(t) = k_2 \exp(-k_1 t)/(k_2 - k_1) - k_1 \exp(-k_2 t)/(k_2 - k_1)$, where k_1 and k_2 are the rate constants of the first and second transition, respectively. When $k_1 = k_2 = k$, $P(t) = (1 + kt) \exp(-kt)$. The flickering in stage R was assumed to be a single pore opening and closing according to kinetics of classical ion channels (Colquhoun and Hawkes, 1983). Thus, open and closed time distributions for
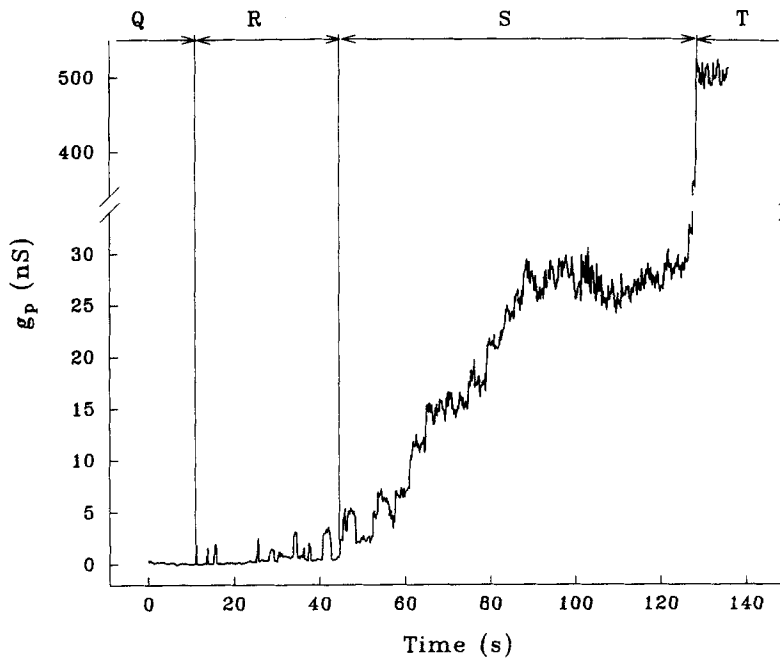

FIGURE 1. Stages of HA mediated cell-planar bilayer fusion. Q, electrically quiescent stage from acidification to the first detected fusion pore. For this example the cis solution was acidified 48 s before the beginning of the record. R, repetitive flickering stage of fusion pore. S, irreversible securely opened pore, characterized by comparably slow pore conductance increases and fluctuations. T, terminal stage of fully opened pore after a stepwise dilation from S. Fusion pore conductance was calculated from ΔY_0. g_p values obtained from ΔY_{90} (not shown) were in agreement with those obtained from ΔY_0.

flickering pores in stage R were fit by the sum of two exponentials using $a_1 \exp(-k_1 t) + a_2 \exp(-k_2 t)$ with $a_1 + a_2 = 1$. For some distributions (e.g., Fig. 9 A), while single exponentials provided reasonable fits, we always used two exponentials to facilitate comparison of distributions obtained under different conditions. Distributions were fit with the nonlinear Marquardt-Levenberg algorithm as implemented in Sigma Plot (version 5.0, Jandel Scientific, Corte Madera, CA). Differences in distributions under altered conditions were evaluated by the nonparametric Kolmogorov-Smirnov test. Distributions were considered statistically different if the attained level of significance was less than 10% ($P < 0.1$). Differences in rate constants were evaluated by a two-tailed t-test. Observed values are presented as mean ± SEM.

RESULTS

The Quiescent Q Stage

When 15–30 cells expressing cleaved HA adhered to the planar membrane bathed by the pH 6.3 solution, the membrane sagged slightly under the weight of the cells. This was hydrostatically compensated by removing solution from the *cis* side (the upper chamber). Within 5–15 s after lowering the pH of the *cis* solution, the planar membrane again sagged, but appreciably more than before, which was relieved by further removing solution from the cis compartment. This indicates that the lowered pH caused the cells to interact with the planar membrane. In control experiments with the HAb2 cell line expressing uncleaved HA0 or with uninfected MDCK cells, sagging did not occur after lowering the pH. Thus, under fusogenic conditions the cleaved HA interacted with the bilayer in the Q stage and reduced the membrane tension before the fusion pore formed. We assessed the kinetics of pore formation from the distributions of waiting times from acidification to the first fusion pore

TABLE I

Rate Constants for Waiting Time Distributions

Stages of fusion	PR8MDCK		J57MDCK
	+Gangl*	−Gangl	+Gangl
Quiescent, Q	0.042 ± 0.001	$0.011 \pm 0.001^{\ddagger}$	$0.029 \pm 0.001^{\ddagger}$
Repetitive flickering, R	0.026 ± 0.001	0.015 ± 0.001	0.032 ± 0.001
Securely open, S	0.015 ± 0.001	0.011 ± 0.001	0.009 ± 0.0004

*+Gangl and −Gangl correspond to ganglioside-containing and ganglioside-free planar bilayers, respectively. ‡Denotes the two equal sequential rate constants. All other distributions were fitted with single exponents. Values are given as mean ± SEM. Rate constants are given in units s^{-1}.

opening, t_Q. The cells were adhered to the planar membrane before acidification and fusion did not occur at neutral pH for as long as 30 min. As low pH initiated the fusion event, t_Q was a direct measure for the time required for the contacting membranes to pass through the multiple steps leading to pore formation.

For simplicity, we denote MDCK cells infected with the PR/8/34 strain of influenza virus as PR8MDCK and MDCK cells infected with the Japan/305/57 strain as J57MDCK. With ganglioside-containing bilayers, t_Q was distributed exponentially (Table I) for PR8MDCK (Fig. 2, *open circles*), indicating that the reactions leading to fusion pore formation could be described by a single rate limiting transition. This distribution was dependent, however, on the strain of virus. For J57MDCK the distribution visually displayed a lag (Fig. 2, *closed circles*), requiring two exponentials for an adequate fit, implying that at least two sequential steps were rate limiting for formation of these fusion pores. That the t_Q distribution were different was affirmed by the nonparametric two-sample Kolmogorov-Smirnov test ($P < 0.01$). We conclude that the kinetics of fusion pore formation for influenza are dependent on the strain of virus.

The Waiting Times of the R and S Stages

The waiting times of t_R and t_S were exponentially distributed for both PR8MDCK and J57MDCK cell-bilayer fusion (Fig. 3). Furthermore, the distributions (e.g., see the rate constants, Table I) displayed little dependence on strain. Thus, unlike the Q stage which was sensitive to the strain of virus (i.e., the amino acid sequence of HA), the latter stages were relatively independent of the strain. The pore left the S stage, and fully opened to the T stage where the pore conductance did not depend on the strain of virus (data not shown).
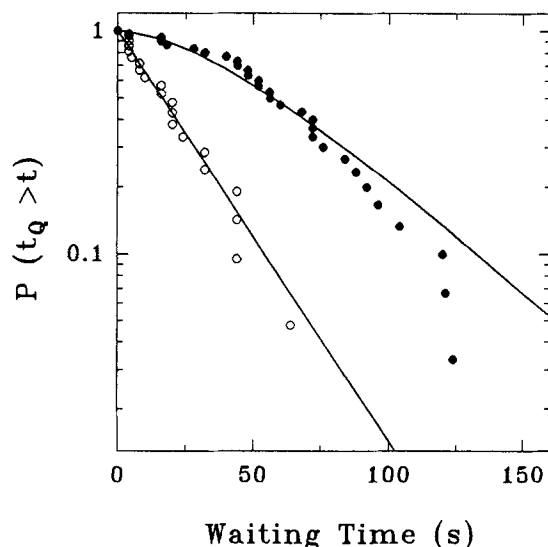

FIGURE 2. Normalized waiting time t_Q distributions for the first detected fusion pores in semilogarithmic scale. In all figures PR8MDCK is shown by open symbols and J57MDCK cells by filled symbols. Nonlinear curve fits are shown by solid lines. Fusion was triggered at time 0 and the waiting time distribution within the Q stage were plotted as the probability that the fusion occurred after time t, $P(t_Q > t)$, as a function of t. For PR8MDCK, the distribution is fit by a single exponential with rate constant 0.042 s^{-1}, ($R^2 = 0.98$, number of points NP = 21). For J57MDCK, two exponentials with equal rate constants of 0.029 s^{-1} provided an optimal fit ($R^2 = 0.97$, NP = 30). When waiting time distribution exhibiting pronounced lags were described by two exponentials, adequate fits were obtained only when the two rate constants were roughly equal. If the constants were markedly different, the predicted distribution showed little lag with the slower rate dominating the exponential decay.

Pore Flickering Within the Reversible R Stage

ΔY_0 *reflects pore flickering.* We established that the repetitive transitions in ΔY_0 (Fig. 4 A) were due to opening and closing of a fusion pore. Clearly, the observed ΔY_0 transitions were due to the fusion pore flickering open and closed when $\Delta Y_{dc} = 0$ (Fig. 4 B) because then $G_m = G_c = 0$ (Melikyan et al., 1993). For some pores, however, $\Delta Y_{dc} \neq 0$. The direct current could, in principle, be flowing through the bilayer conductance, G_m, unrelated to fusion, or through the pore, g_p, and cell membrane, G_c (Fig. 4 B). (We assumed that current did not flow through the walls of the fusion pore.)

We directly established that flickering in ΔY_0 was due to fusion by performing experiments with low frequency (≈ 100 Hz) stimulating sinusoidal voltages where

A

B

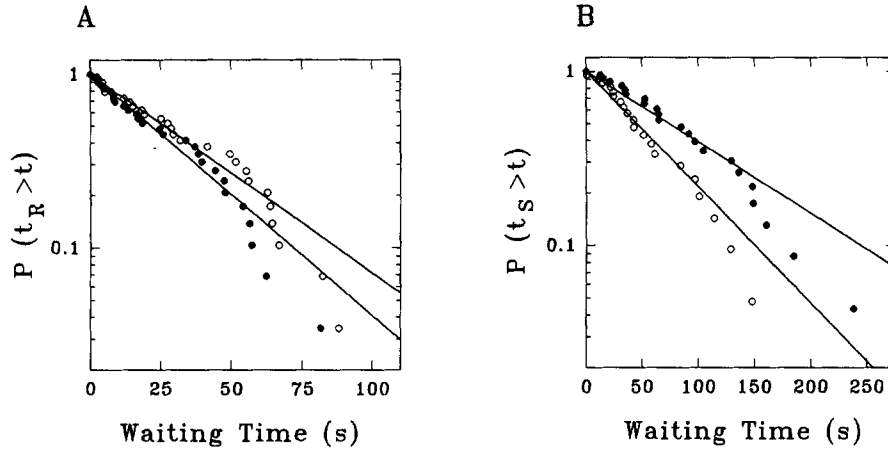Waiting Time (s)   Waiting Time (s)

FIGURE 3.   Normalized waiting time distributions (A) for the repetitive flickering stage, t_R, and (B) for the securely open stage, t_S. t_R and t_S were fit by single exponentials with rate constants $k_R = 0.026$ s^{-1} ($R^2 = 0.98$, NP $= 29$), $k_S = 0.015$ s^{-1} ($R^2 = 0.98$, NP $= 21$) for PR8MDCK (*open circles*) and $k_R = 0.032$ s^{-1} ($R^2 = 0.99$, NP $= 29$), $k_S = 0.009$ s^{-1} ($R^2 = 0.97$, NP $= 23$) for J57MDCK (*filled circles*).
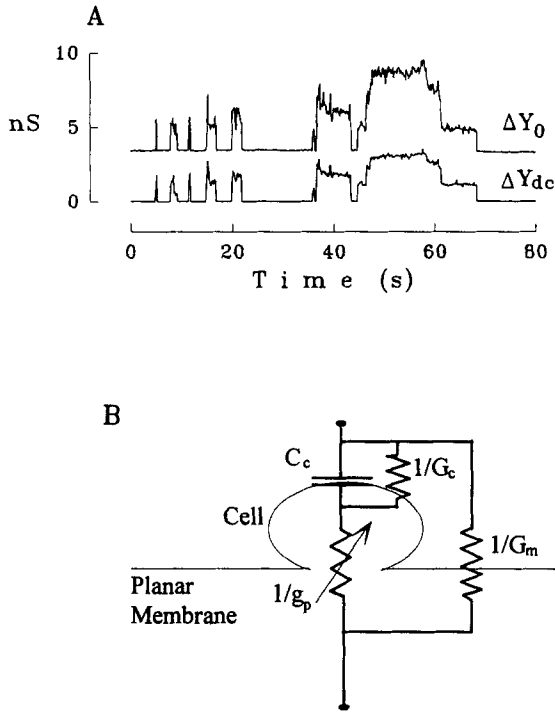
A

B

FIGURE 4.   (A) Typical example of fusion pore flickering within R stage for J57MDCK fusion to planar bilayer. ΔY_0 is displaced upward for visual clarity. ΔY_0 and ΔY_{dc} change in concert, with ΔY_0 exhibiting the larger changes. (B) Equivalent circuit of cell-bilayer fusion. G_c and C_c are the cell membrane conductance and capacitance, respectively. g_p is the fusion pore conductance and G_m is the planar bilayer conductance. When the dc current pathway is through g_p and G_c, and not through G_m, $\Delta Y_0 > \Delta Y_{dc}$ as in A. The capacitance of the planar membrane was compensated throughout the experiment and is not shown.

small pore conductances were detected by ΔY_{90}. Here, virtually all early ΔY_0 fluctuations were accompanied by ΔY_{90} fluctuations followed by complete pore opening, regardless of the magnitude of the ΔY_{dc} changes. This shows that the currents were through the fusion pore. We did not, however, routinely use low frequency measurements because higher frequencies provided larger signal/noise ratios and greater time resolutions enabling detection of smaller pores. (Also, the higher cell admittance allowed the final pore conductance to be determined.) We checked that when higher (e.g., 800 Hz) frequencies were used and, therefore, smaller pores detected, the ΔY_0 fluctuations were due to fusion pore flickering when $\Delta Y_{dc} \neq 0$.

As shown in Fig. 4 A, ΔY_{dc} fluctuations usually followed the same pattern as ΔY_0. Because in this case the reversible changes in ΔY_{dc} synchronized with ΔY_0, we assumed the fluctuations reflected dc currents through either g_p in series with G_c or through G_m, but not both of these independent pathways. (All electrical changes, ΔY_{90}, ΔY_0, and ΔY_{dc}, were due to cleaved HA-bilayer interactions under fusogenic conditions [Melikyan et al., 1993].) We showed that the fluctuations in ΔY_0 (Fig. 5, A and B) were due to opening and closing of the fusion pore by measuring the ratio $\Delta Y_0 / \Delta Y_{dc}$ for a set of flickers. The rationale was that $\Delta Y_0 = \Delta Y_{dc}$ if the dc current is through the bilayer, whereas $\Delta Y_0 > \Delta Y_{dc}$ if the current is through the pore, assuming that G_c is not much greater than g_p.[1] We verified the experimental reliability of the approach by incorporating VDAC into bilayers: $\Delta Y_0 / \Delta Y_{dc}$ was measured as 0.98 ± 0.04 ($n = 10$), in accord with the theoretical expectation of 1.0 when current can be only through the bilayer. The $\Delta Y_0 / \Delta Y_{dc}$ histograms for flickers (Fig. 5 C for PR8MDCK, and D for J57MDCK) show that ΔY_0 was characteristically larger than ΔY_{dc} when the two flickered in tandem. The ratio was 1.90 ± 0.12 ($n = 39$) for PR8MDCK and 1.58 ± 0.07 ($n = 35$) J57MDCK, verifying that ΔY_0 current was through the pore. The test was further checked by noting that when $G_c \gg g_p$, $\Delta Y_0 / \Delta Y_{dc}$ would equal one (even if $G_m = 0$). We created this case by using saponin to make PR8MDCK cells permeable. $\Delta Y_0 / \Delta Y_{dc}$ was reduced to 1.1 ± 0.05 ($n = 10$, range 0.9 to 1.4) and the histogram of this ratio (Fig. 5 C, hatched bars) was substantially shifted to values around 1. The largest ratios probably occurred for cells not made sufficiently permeable (see Materials and Methods). Having established that flickering of ΔY_0 was due to flickering in g_p, the independent measurements of ΔY_0 (Figs. 5, A and B) and ΔY_{dc} determined G_c.[1] The calculated values of G_c varied from 1 to 15

---

[1] Qualitatively, the cell is electrically transparent to 800 Hz sinewaves (ωC_c is large), but resistive to dc current. Thus, the sinusoidal voltage drops entirely across g_p (and not across G_c). Quantitatively,

$$Y_0 = \frac{G_m + G_c(1 + G_c/g_p) + \omega^2 C_c^2/g_p}{(1 + G_c/g_p)^2 + (\omega C_c/g_p)^2},$$

$$Y_{90} = \omega C_m + \frac{\omega C_c}{(1 + G_c/g_p)^2 + (\omega C_c/g_p)^2},$$

and $Y_{dc} = G_m + g_p G_c/(g_p + G_c)$.

For $g_f \ll \omega C$, $Y_0 = g_p + G_m$. Thus, if Y_0 is due to current through g_p and G_c (and not G_m), the combination of Y_0 and Y_{dc} determines g_p and G_c.

nS with a mean of around 4 nS for both virus strains under fusogenic conditions. This is similar to the observed increases in G_c for HAb2 cells at acidic pH (Spruce et al., 1989).

The kinetics of flickering within the R stage. The flickering pores exhibited instantaneous transitions between open and closed states (≈ 15 ms to rise from 10–90% of final value, limited by time resolution of admittance measurement).
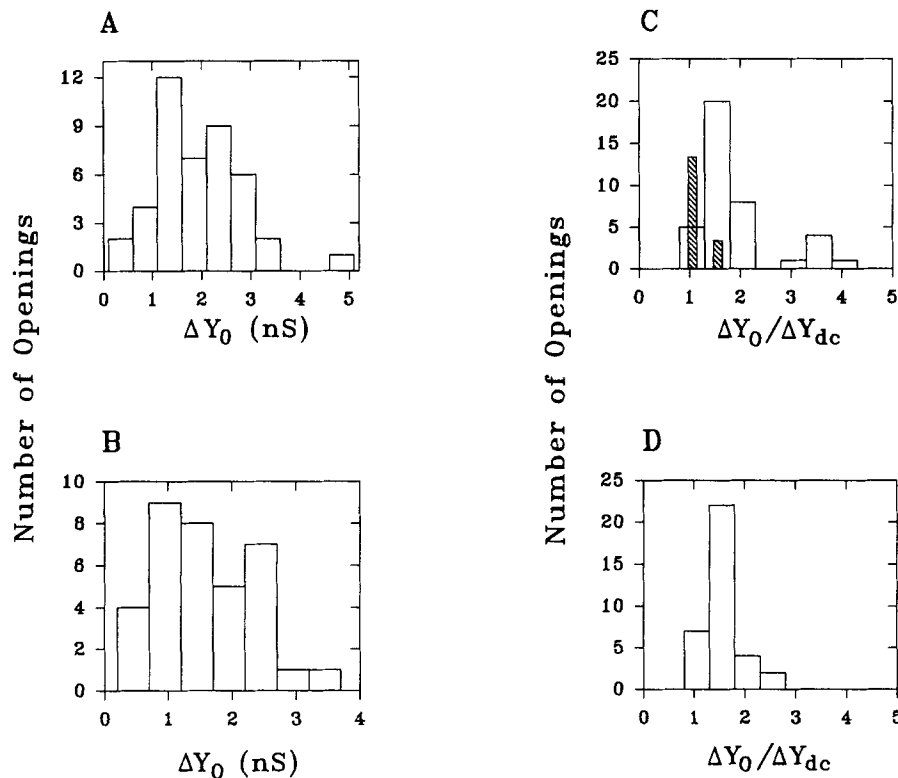

FIGURE 5.   Pore conductance distribution, ΔY_0, and $\Delta Y_0/\Delta Y_{dc}$ histograms in the R stage for PR8MDCK (A and C) and J57MDCK cells (B and D). ΔY_0 of the flickering pore was calibrated in units of nS. The parallel ΔY_{dc} changes were monitored (see for example Fig. 4) and the resulting $\Delta Y_0/\Delta Y_{dc}$ ratios are shown. Hatched bars (C) correspond to PR8MDCK cells made permeable by saponin, so $G_c > g_p = \Delta Y_0$ for the flickering pores. For A, $n = 43$ openings for $N = 8$ cells; (B and D) $n = 35$, $N = 7$; (C) $n = 39$, $N = 7$. For the hatched histogram of C, $n = 10$, $N = 3$.

Within our resolution, the rise times were identical to those of VDAC channels. Because openings and closings of fusion pores were reminiscent of the kinetic behavior of single ion channels, we analyzed the open and closed time distributions for fusion pores during the flickering stage as if they were channels transiting between defined states. Both the open (Fig. 6) and closed (Fig. 7) time distributions of PR8MDCK and J57MDCK cells were characterized by two rate constants (Table
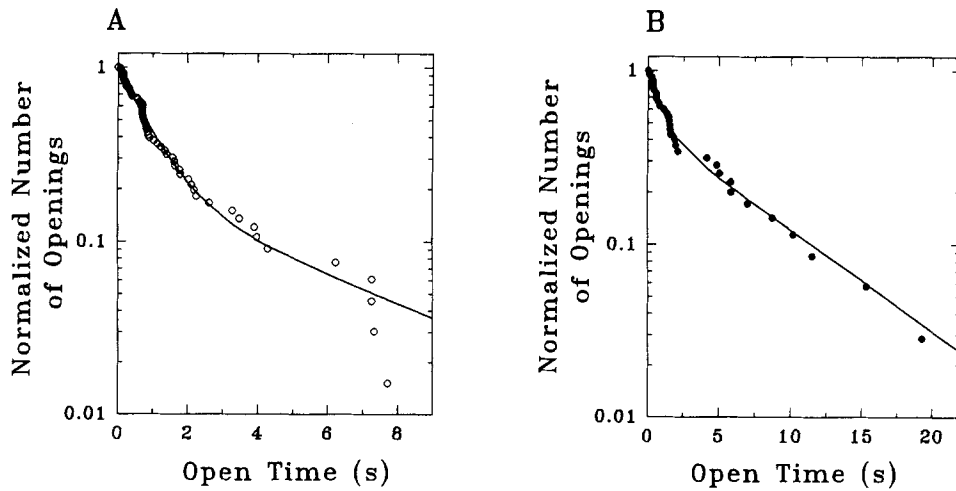
A   B

FIGURE 6. Normalized open time distributions for fusion pore flickering. (A) PR8MDCK. (B) J57MDCK. Each open time in the R stage was measured from ΔY_0. Data were fit by the sum of two exponentials with: k_1 = 1.12, k_2 = 0.19 s^{-1}, weighting coefficients a_1 = 0.8, a_2 = 0.2 for PR8MDCK (R^2 = 0.99, NP = 66) and k_1 = 1.11, k_2 = 0.14 s^{-1}, a_1 = 0.53, a_2 = 0.47 (R^2 = 0.99, NP = 35) for J57MDCK.

II). While the corresponding distributions were qualitatively the same for the two strains of virus, the rate constants and weighting coefficients exhibited quantitative differences. For instance, pores for PR8MDCK cells tended to have shorter open times.
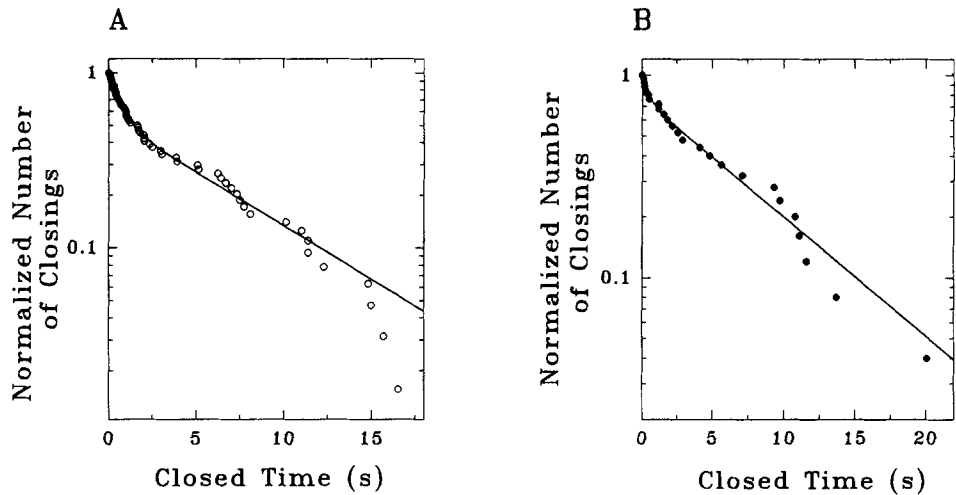
A   B

FIGURE 7. Normalized closed time distributions for flickering pores in the R stage. (A) PR8MDCK. (B) J57MDCK. The time intervals between the last closures and the beginning of the S stages are included in the distributions. The non-linear curve fit using the sum of two exponentials gave: k_1 = 1.46 s^{-1}, k_2 = 0.14 s^{-1}, a_1 = 0.45, a_2 = 0.55 (R^2 = 0.99, NP = 64) for PR8MDCK and k_1 = 2.87, k_2 = 0.14 s^{-1}, a_1 = 0.23, a_2 = 0.77 (R^2 = 0.99, NP = 25) for J57MDCK.

Influence of Target Membrane on the Fusion Pore Characteristics

We included gangliosides in the planar membrane because HA binds to their terminal sialates. Gangliosides are thus often referred to as receptors for HA (Suzuki, Nagao, Kato, Matsumoto, Nerome, Nakajima, and Nobusawa, 1986). The efficiency of fusion increased by incorporating gangliosides in the planar membrane. In their presence, 10–15% of the adherent cells fused with the pore fully opening. In the absence of gangliosides, only ≈1% of the adherent cells from the same infected batches fused and exhibited pores that reached the *T* stage. The presence of gangliosides also affected the kinetics for the formation and the subsequent enlargement of the pores.

Whereas the waiting time distribution, t_Q, for PR8MDCK cells in the presence of gangliosides was exponentially distributed (Fig. 2), in the absence of gangliosides there was a pronounced lag (Fig. 8 *A*). As readily seen by comparing Figs. 2 and 8 *A*, fusion was drastically slowed by omitting gangliosides. With gangliosides, 67% of the

TABLE II

Rate Constant of Flickering Fusion Pore

Pore State	PR8MDCK(+G)*	PR8MDCK(−G)	PR8MDCK(+G)+C‡	J57MDCK(+G)
Open				
k1	1.12 ± 0.11	1.51 ± 0.47	2.88 ± 0.70	1.11 ± 0.19
k2	0.19 ± 0.08	0.28 ± 0.04	0.51 ± 0.58	0.14 ± 0.02
a1	0.80 ± 0.07	0.34 ± 0.09	0.81 ± 0.19	0.53 ± 0.06
a2	0.20 ± 0.08	0.66 ± 0.10	0.19 ± 0.20	0.47 ± 0.06
Closed				
k1	1.46 ± 0.11	0.55 ± 0.05	2.93 ± 0.79	2.87 ± 0.86
k2	0.14 ± 0.01	0.05 ± 0.01	0.68 ± 0.10	0.14 ± 0.01
a1	0.45 ± 0.02	0.72 ± 0.04	0.38 ± 0.11	0.23 ± 0.03
a2	0.55 ± 0.02	0.28 ± 0.04	0.62 ± 0.11	0.77 ± 0.02

*+G and −G stand for ganglioside-containing and ganglioside-free planar bilayers, respectively.

‡+C denotes cells treated with colchicine and cytochalasin B. Rate constants are in units of s^{-1}.

cells have fused by 20 s; without gangliosides the cells were still in the lag phase. Even after the lag phase, the rate of fusion was significantly less without gangliosides. The t_Q distribution for PR8MDCK cells in the absence of gangliosides could be fit with a sequential two transition model. The lag and final slope were optimally fit when the two rate constants were set equal. The slowing of fusion in the absence of gangliosides is reflected in the need for two steps, rather than one, to describe the kinetics and the values of the rate constants (Table I): the two equal rate constants were a factor of four less than the single rate constant for PR8MDCK in the presence of gangliosides. The statistical distribution of the waiting times was altered by gangliosides and was not a consequence of the fit (Kolmogorov-Smirnov $P < 0.01$). Thus, the kinetics for the formation of the pore were significantly controlled by gangliosides.

The presence of gangliosides was not as consequential for the *R* and *S* stages. The waiting time distribution of the *R* stage remained a single exponential in the absence of gangliosides (Fig. 8 *B*), although the rate constant was reduced by a factor of two (Table I). Omitting the gangliosides did not alter the open (Fig. 8 *C*) or closed time

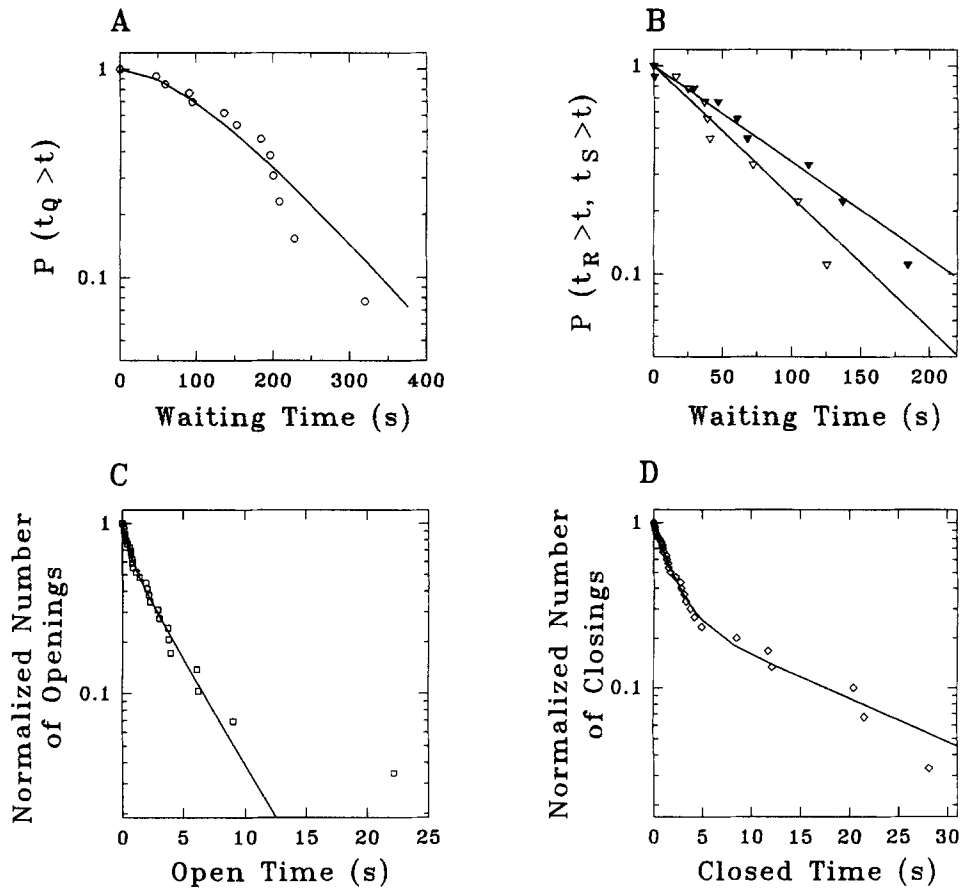

FIGURE 8. Fusion pore characteristics in the absence of gangliosides. All experiments were performed with PR8MDCK cells and DOPC/PE (2:1) bilayers. (A) The normalized waiting time distribution, t_Q, (*open circles*) qualitatively differed from ganglioside-containing bilayer distribution (see Fig. 2) and was fit by two sequential and equal rate transitions with $k_1 = k_2 = 0.011$ s^{-1} ($R^2 = 0.96$, NP = 13). (B) t_R (*open triangles*) and t_S (*filled triangles*) distributions fit by single exponentials with rate constants of 0.015 s^{-1} ($R^2 = 0.96$, NP = 9) and 0.011 s^{-1} ($R^2 = 0.97$, NP = 9), respectively. (C) Normalized fusion pore open time distribution during flickering (*open squares*) fit by the sum of two exponentials with $k_1 = 1.51$ s^{-1}, $k_2 = 0.28$ s^{-1}, $a_1 = 0.34$, $a_2 = 0.66$ ($R^2 = 0.99$, NP = 29). (D) Normalized flickering pore closed time distribution (*open diamonds*). Solid line represents a non-linear fit as in C with $k_1 = 0.55$ s^{-1}, $k_2 = 0.05$ s^{-1}, $a_1 = 0.72$, $a_2 = 0.28$ ($R^2 = 0.99$, NP = 30).

distributions of the flickering pore (Fig. 8 D) by the Kolmogorov-Smirnov test and both distributions were fit by a sum of two exponentials (Table II). While the open time rate constants were not changed by omitting gangliosides, pores with the longer open time occurred more frequently (i.e., a_2 increased when omitting gangliosides). Also, the two closed rate constants decreased (i.e., the lifetimes of each closed state increased) and the state with shorter closed times became more prevalent when gangliosides were omitted.

While pores of the first fusing cell invariably showed the four stage behavior with gangliosides, without gangliosides pores sometimes never entered the T stage for as long as we tested, up to 15 min. (As we followed these admittances for inordinantly long times, ΔY_{dc} often increased greatly, contaminating the ΔY_0 signal. It is possible that the pore did not even remain open. If $g_p > 50$ nS, at 800 Hz the ΔY_{90} signal was large enough to follow fluctuations in the conductance of fusion pores. For $g_p < 20$ nS, ΔY_{90} was not sufficiently sensitive to detect pores.) We generated the t_S distribution from only those pores that clearly left the S stage for the T stage with the diagnostic rapid increase in g_p (Fig. 1). For this subset of pores, the distribution was fit by a single exponential with statistically the same rate constant as that obtained with gangliosides (Table I).
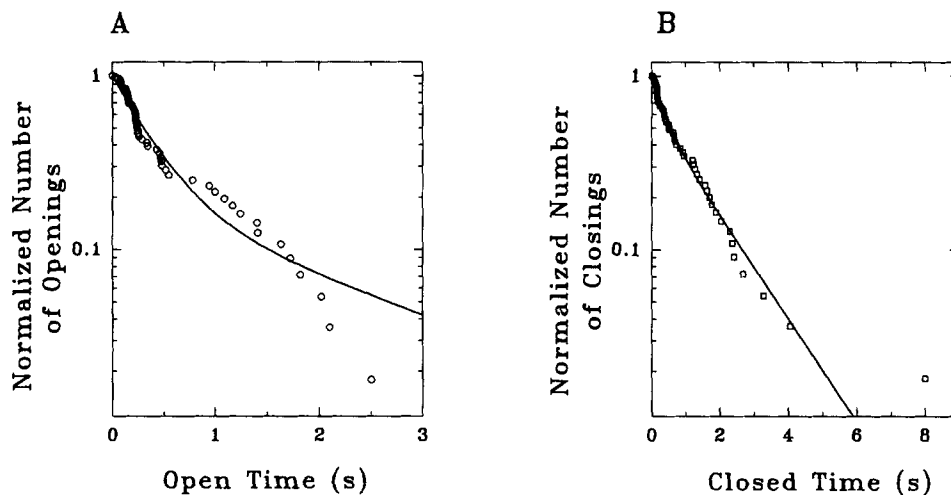

FIGURE 9. The influence of colchicine and cytochalasin B on the fusion pore properties of PR8MDCK cells. (A) Normalized flickering fusion pore open time distribution in R stage (*open circles*) fit by the sum of two exponentials with $k_1 = 2.88$, $k_2 = 0.51$ s^{-1}, $a_1 = 0.81$, $a_2 = 0.19$ ($R^2 = 0.96$, NP = 56). (B) Normalized closed time distribution (*open squares*). Solid line shows an optimal fit with $k_1 = 2.93$ s^{-1}, $k_2 = 0.68$ s^{-1}, $a_1 = 0.38$, $a_2 = 0.62$ ($R^2 = 0.99$, NP = 55).

Cell Cytoskeleton Does Not Exert Large Control on the Pore

Because it was conceivable that constraints imposed by the cytoskeleton might affect the formation or growth of fusion pores, we treated PR8MDCK cells with colchicine and cytochalasin B to disrupt the tubulin and actin portions of the cytoskeleton. This treatment did not alter the latencies from acidification to fusion: the t_Q waiting time distribution, with ganglioside-containing membranes, was not affected by the treatment. However, the parameters needed to fit the open and closed time distributions were changed (Fig. 9, Table II). The pore flickered faster with more and shorter openings and closings: disruption of cytoskeleton increased the average number of pore flicker events from 5 to 12 before irreversible opening to the S stage. Also after treatment, there was less need for two exponentials to fit the open and closed time

distributions; they could be reasonably fit by single exponentials. But the treatment did not statistically change the open or closed time distributions within the R stage as evaluated by the Kolmogorov-Smirnov test (data not shown). The conductances, g_p, of the flickering pore were not statistically altered by disrupting the cytoskeleton. Despite changes in individual rate constants and their relative weights, the fitted distributions indicate that the open to closed time ratio was not significantly altered by treating cells with the cytoskeletal agents.

DISCUSSION

The Lag Time Before Fusion

Attempts have been made to dissect the steps leading to fusion (Blumenthal et al., 1991), with particular attention paid to the lag time from acidification to fusion (Morris, Sarkar, White, and Blumenthal, 1989; Clague et al., 1991; Bentz, 1992). When populations of fusion events are studied, lag times between acidification and the onset of fusion are observed. This time can be set independent of sensitivity of measurement when characteristic sigmoidal-shaped signals for fusion as a function of time are obtained (Bentz, 1992). When fusion is observed on the level of individual events, the time courses for fusion as would be observed in population studies are easily produced by accumulating data for many events. It should be realized that "waiting time" from acidification to a single fusion event is not synonymous with lag time. For example, a process described by a single exponential does not have a lag time, but there is a waiting time for any particular event. We use the term lag time to denote that waiting time distributions are not exponentially distributed (e.g., see Fig. 2, closed circles). Our lag times correspond to those obtained from the sigmoidal time courses of fusion observed in population studies.

Whereas early reports of populations of intact virions (including Japan 57, PR8, and X-47 strains) fusing to red blood cell membranes showed minimal or no lags (Stegmann et al., 1986; Morris et al., 1989), more recent stopped-flow experiments (using X-31 strain) with their faster time resolutions revealed definite pH-dependent lags (Clague et al., 1991). Systematic studies of fusion of cells expressing the Japan 57 strain of HA to red blood cells showed that lags varied inversely with the density of active HA, altered by varying the percentage of HA0 precursors activated by proteolytic cleavage (Clague et al., 1991). As yet undefined physical properties of the host membranes also affected the lags in those studies. It was suggested that lags were caused by the time required for HA-trimers, at lower densities on cell surfaces, to laterally associate (Morris et al., 1989; Ellens, Bentz, Mason, Zhang, and White, 1990; Clague et al., 1991). For fusion of individual fibroblasts, transfected with the gene of Japan 57 strain of HA, to erythrocytes, pronounced lags were again found (Kaplan, Zimmerberg, Puri, Sarkar, and Blumenthal, 1991; Spruce et al., 1989), similar to what we observed on the bilayer system. (Time courses of individual fusions of cells expressing HA from other strains of influenza have not been reported to our knowledge.) Our preliminary measurements with these transfected lines show similar waiting time distributions for fusion to planar membranes (data not shown), although longer lags were observed with planar membranes.

Our results call into question the universality of the lag phenomenon. Structural details of HA are important for the very existence of the phenomenon: whereas

J57MDCK cells exhibited a lag, PR8MDCK did not. The absence of a lag with PR8MDCK appears to be a property of HA and not that they are expressed in cells: waiting times for fusion of PR8 (and Ukraine/1/63) strain of virus to ganglioside-containing planar membranes were also exponentially distributed (Niles, Li, and Cohen, 1992; Niles and Cohen, 1993). Because the lag is somewhat longer for HAb2 cells fusing to bilayers (data not shown) than fusing to erythrocytes (Spruce et al., 1989), the absence of a lag in the PR8MDCK studies is significant.

Fusion kinetics have been determined by dequenching of membrane fluorescent probes resulting from populations of virus fusing to host membranes. Specific models were fitted to the resulting macroscopic fluorescence increases to obtain binding and fusion rate constants (Nir, Stegmann, and Wilschut, 1986; Bentz, 1992). Although it has been argued that dye redistribution is sufficiently fast to accurately report fusion kinetics (Chen and Blumenthal, 1989), simultaneous dye and patch clamp measurements indicate that dye does not spread from erythrocytes to HA-expressing cells if the pore remains small (Tse, Iwata, and Almers, 1993). Dye dispersal becomes increasingly faster as the pore enlarges. Also, whereas release of dye from virus to red cells is anomalously slow (Georgiou, Morrison, and Cherry, 1989; Lowy, Sarkar, Chen, and Blumenthal, 1990), release from virus into planar membranes is as expected from diffusion (Niles and Cohen, 1991a). Because the kinetics of dye release depends on the target membrane, dye spread may not reflect the true fusion kinetics. Fusion kinetics will be best determined on the level of individual events.

Later Stages of the Pore

Once the pore was formed, the strain of virus did not have much effect on the growth of the pore. The waiting time distributions for the R and S stages were essentially the same for both strains (Fig. 3). Thus, structural differences between HA trimers appear important for the conformational changes, aggregation, and membrane destabilizations required for fusion pore formation (Blumenthal et al., 1991), but are of relatively minor importance for its subsequent evolution. The HA structure may, however, influence the flickering rate of pores during the R stage, as longer openings were more probable for J57MDCK (Fig. 7; Table II). The structural differences in HA did not alter the initial pore conductances (1.93 ± 0.13 nS for PR8MDCK versus 1.64 ± 0.13 nS for J57MDCK). Also, for both strains of virus, scattergrams indicate that the magnitude of pore conductances did not correlate with their open times (data not shown).

It was estimated from the submillisecond time courses of charging the capacitance of erythrocyte membranes through the fusion pores connecting them to HAb2 cells that pores opened with ≈ 150 pS conductances (Spruce et al., 1991). These pores enlarged to 500–600 pS by the time they could be detected by time-resolved admittance measurements (Spruce et al., 1989, 1991). It is possible that in the bilayer system, pores opened with these smaller conductances and the tension of the bilayer enlarged the pores before we could detect them (noise = 0.2 pA rms at 200 Hz). On the other hand, differing pore conductances could occur for other reasons. For instance, pore lengths are unknown and could vary between systems: the glycocalyces of erythrocytes could cause their pores to be longer than those of bilayers. Pore lengths on the order of 200 nm (rather than 15 nm [Spruce et al., 1989]) were detected by EM for HA-expressing cells fused to erythrocytes (Doxsey, Sambrook,

Helenius, and White, 1985). In the bilayer system, the 2 nS pores seen in the R stage correspond to diameters of ~6–7 nm, assuming a length of 15 nm. This suggests that the flickering pores are either purely lipidic (Stegmann et al., 1990; Siegel, 1993; Nanavati, Markin, Oberhauser, and Fernandez, 1992) or a lipid-protein structure (Zimmerberg, Curran, and Cohen, 1991), rather than purely protein (Almers and Tse, 1990).

Influence of the Target Membrane

For fusion of influenza virus to lipid vesicles, the phospholipid composition is not critical and the importance of HA receptors, in the form of gangliosides, has been considered minor (White et al., 1982; Stegmann, Nir, and Wilschut, 1989; Stegmann et al., 1990). However, for PR8 fusion to liposomes (at 37°C), gangliosides increased the rate of fusion by a factor of 30 (Wunderli-Allenspach and Ott, 1990). Also, lags were reduced from 30 min in the absence of gangliosides to 4–8 min in their presence when X-31 strain of virus fused to vesicles at 0°C (Stegmann et al., 1990). When influenza virus fused to planar membranes, the effects of gangliosides were unambiguous (Niles and Cohen, 1991b). In the presence of gangliosides, waiting time distributions of individual virion fusion events were exponentially distributed whereas in their absence the distributions were complex (Niles and Cohen, 1993). In this paper we showed that in the cell-planar membrane system, the gangliosides again significantly altered the waiting time distribution from acidification to fusion. For PR8MDCK cells, a long lag time was eliminated with gangliosides (Figs. 2 and 9). The gangliosides must be altering the fusion process, not merely increasing binding, because the exponential fall in the waiting time distribution after the lag without gangliosides is significantly less steep than the fall with gangliosides (Table I). Also, the gangliosides ensured that pores reached the T stage. It should not be surprising that the functional properties of HA are altered upon binding the small ligand sialate: it is generally the rule that small ligands activate large membrane protein receptors.

Whereas gangliosides substantially altered the t_Q distribution, they influenced the kinetics of pore flickering and the t_R distribution to only a small degree (Figs. 7 and 9). Without gangliosides, the pore did not necessarily leave the S stage. However, when it did the t_S distributions were the same. In other words, gangliosides insured that pores fully enlarged without altering the pore behavior within the R or S stages.

Growth from a small initial pore to a larger pore is seen in fusion of HA-expressing cells to erythrocytes (Spruce et al., 1989, 1991) and in exocytotic release from mast cells (Zimmerberg et al., 1987; Breckenridge and Almers, 1987; Spruce et al., 1989, 1991; Curran et al., 1993). In these systems, a single flicker (an opening and closing) can be seen before the pore irreversibly opens. Generally, repetitive flickering does not occur. In HA-induced cell-bilayer fusion, repetitive flicker before the pore securely opens is almost always the case.

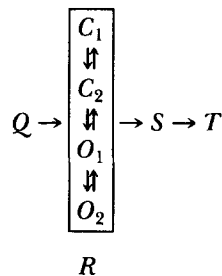### The Utility of Describing Fusion by Sequential Stages

Fusion pores were shown to grow in stages for exocytotic secretion from mast cells, although the flickering stage, seen in the cell-planar bilayer system, was rare (Curran et al., 1993). We classified stages based on obvious visual characteristics of conductances. While our classification is purely phenomenological, the surprisingly simple

forms exhibited by the waiting time distributions indicate that the classification of pore activity by sequential stages has quantitative utility. The effects of experimental manipulations (i.e., varying strain of virus, including gangliosides, disrupting cytoskeleton) on the formation and evolution of fusion pores could be quantified from the waiting time distributions characterizing each stage. In spite of this utility, it does not follow that pore growth truly follows sequential stages. Also, the flickering associated with the R stage of a second pore could be occurring during the S stage of the first pore (e.g., see Fig. 1). Furthermore, uncertainties in the transition from the R to S stage could corrupt waiting times. For example, increases in G_m would result in increases in Y_o (Fig. 4 B) which would overestimate the duration of the S stage. In fact, correcting preliminary measurements with HAb2 cells for this leakage indicate that the S stage is on the order of 10 s rather than the uncorrected 100 s (Fig. 3 B).

Transitions Within Stages

We interpreted exponentially-distributed waiting times of the electrically quiescent Q stage as indicating a single rate limiting step from acidification to fusion. However, the multiple conductance states within both the R and S stages calls into question the interpretation of apparent single exponential waiting time distributions as implying single rate limiting steps.

The flickering within the R stage may be a side reaction, unrelated to the pore actually enlarging from the R to S stage. For instance, consider

$$Q \rightarrow \begin{array}{|c|} \hline C_1 \\ \Updownarrow \\ C_2 \\ \Updownarrow \\ O_1 \\ \Updownarrow \\ O_2 \\ \hline \end{array} \rightarrow S \rightarrow T$$

$$R$$

where the open and closed states of R have been placed in an arbitrary sequence. If a larger activation barrier separates the R and S stages when cells fuse to bilayers than when they fuse to erythrocytes, due to any differences such as pore geometry, repetitive pore flickering would occur and a single exponential distribution would result naturally for the $R \rightarrow S$ transition. However, as the rate constants for transiting between the flickering open and closed states are sufficiently large with respect to the time spent in the R stage and the t_R distributions are not perfect exponentials (Fig. 3), the alternative possibility that the pore sequentially passes through multiple open and closed states before securely opening cannot be dismissed. Independent of whether flickering is a side reaction, we thus picture relatively low energy barriers separating the various open and closed states with any two sequential states having comparable energies.

The conductances of pores were not stereotypic in the S stage. There was a continuum of conductance values, from 2 to 100 nS, for pores in this stage. Pores thus pass through a large number of conducting states before exiting this stage.

Either there is a true rate limiting step or multiple steps combine to an apparent single exponential.

The effects of virus strain and presence of gangliosides were most pronounced during the formation of the pore. Accordingly, we propose that, in general, the kinetics of pore formation depend on the fusion proteins in the virus and their receptors in the target membrane; once the pore has formed, fusion proteins have relatively little importance for subsequent growth of the pore.

REFERENCES

Almers, W., and F. W. Tse. 1990. Transmitter release from synapses: does a preassembled fusion pore initiate exocytosis? *Neuron.* 4:813–818.

Alvarez de Toledo, G., and J. M. Fernandez. 1988. The events leading to secretory granule fusion. *In* Cell Physiology of Blood. R. B. Gunn and J. C. Parker, editors. The Rockefeller University Press, New York. 333–344.

Bentz, J. 1992. Intermediates and kinetics of membrane fusion. *Biophysical Journal.* 63:448–459.

Blumenthal, R., C. Schoch, A. Puri, and M. J. Clague. 1991. A dissection of steps leading to viral envelope protein-mediated membrane fusion. *In* Calcium Entry and Action at the Presynaptic Nerve Terminal. Annals of the New York Academy of Sciences, 635:285–296.

Breckenridge, L. J., and W. Almers. 1987. Final steps in exocytosis observed in a cell with giant secretory granules. *Proceedings of the National Academy of Sciences, USA.* 84:1945–1949.

Chen, Y.-D., and R. Blumenthal. 1989. On the use of self-quenching fluorophores in the study of membrane fusion kinetics. The effect of slow probe redistribution. *Biophysical Chemistry.* 34:283–292.

Clague, M. J., C. Schoch, and R. Blumenthal. 1991. Delay time for influenza virus hemagglutinin-induced membrane fusion depends on hemagglutinin surface density. *Journal of Virology.* 65:2402–2407.

Colquhoun, D., and A. G. Hawkes. 1983. The principles of the stochastic interpretation of ion-channel mechanisms. *In* Single Channel Recording. B. Sakmann and E. Neher, editors. Plenum Publishing Corp. New York. 135–175.

Colombini, M. 1989. Voltage gating in the mitochondrial channel, VDAC. *Journal of Membrane Biology.* 111:103–111.

Curran, M., F. S. Cohen, D. E. Chandler, P. J. Munson, and J. Zimmerberg. 1993. Exocytotic fusion pores exhibit semi-stable states. *Journal of Membrane Biology.* 133:61–75.

Doms, R. W., and A. Helenius. 1986. Quaternary structure of influenza virus hemagglutinin after acid treatment. *Journal of Virology.* 60:833–839.

Doms, R. W., A. Helenius, and J. M. White. 1985. Membrane fusion activity of the influenza virus hemagglutinin (the low pH-induced conformational change). *Journal of Biological Chemistry.* 260:2973–2981.

Doxsey, S. J., J. Sambrook, A. Helenius, and J. M. White. 1985. An efficient method for introducing macromolecules into living cells. *Journal of Cell Biology.* 101:19–27.

Ellens, H., J. Bentz, D. Mason, F. Zhang, and J. M. White. 1990. Fusion of influenza hemagglutinin-expressing fibroblasts with glycoprotein-bearing liposomes: role of hemagglutinin surface density. *Biochemistry.* 29:9697–9707.

Georgiou, G. N., I. E. G. Morrison, and R. J. Cherry. 1989. Digital fluorescence imaging of fusion of influenza virus with erythrocytes. *FEBS Letters.* 250:487–492.

Gething, M.-J., and J. Sambrook. 1982. Construction of influenza haemagglutinin genes that code for intracellular and secreted forms of the protein. *Nature.* 300:598–603.

Harter, C., P. James, T. Bachi, G. Semenza, and J. Brunner. 1989. Hydrophobic binding of the ectodomain of influenza hemagglutinin to membranes occurs through the "fusion peptide." *Journal of Biological Chemistry.* 264:6459–6464.

Kaplan, D., J. Zimmerberg, A. Puri, D. P. Sarkar, and R. Blumenthal. 1991. Single cell fusion events induced by influenza hemagglutinin: Studies with rapid-flow, quantitative fluorescence microscopy. *Experimental Cell Research.* 195:137–144.

Lowy, R. J., D. P. Sarkar, Y. Chen, and R. Blumenthal. 1990. Observation of single influenza virus-cell fusion and measurement by fluorescence video microscopy. *Proceedings of the National Academy of Sciences.* 87:1850–1854.

Melikyan, G. B., W. D. Niles, M. E. Peeples, and F. S. Cohen. 1993. Influenza hemagglutinin-mediated fusion pores connecting cells to planar membranes: flickering to final expansion. *Journal of General Physiology.* 102:1151–1170.

Monck, J. R., G. Alvarez de Toledo, and J. M. Fernandez. 1990. Tension in secretory granule membranes causes extensive membrane transfer through the exocytotic fusion pore. *Proceedings of the National Academy of Sciences, USA.* 87:7804–7808.

Morris, S. J., D. P. Sarkar, J. M. White, and R. Blumenthal. 1989. Kinetics of pH-dependent fusion between 3T3 fibroblasts expressing influenza hemagglutinin and red blood cells. *Journal of Biological Chemistry.* 264:3972–3978.

Nanavati, C., V. S. Markin, A. F. Oberhauser, and J. M. Fernandez. 1992. The exocytotic fusion pore modeled as a lipidic pore. *Biophysical Journal.* 63:1118–1132.

Niles, W. D., and F. S. Cohen. 1991a. Fusion of influenza virions with a planar lipid membrane detected by video fluorescence microscopy. *Journal of General Physiology.* 97:1101–1119.

Niles, W. D., and F. S. Cohen. 1991b. The role of N-acetylneuraminic (sialic) acid in the pH dependence of influenza virion fusion with planar phospholipid membranes. *Journal of General Physiology.* 97:1121–1140.

Niles, W. D., and F. S. Cohen. 1993. Single event recording shows that receptor docking alters the kinetics of membrane fusion mediated by influenza hemagglutinin. *Biophysical Journal.* 65:171–176.

Niles, W. D., Q. Li, and F. S. Cohen. 1992. Computer detection of the rapid diffusion of fluorescent membrane fusion markers in images observed with video microscopy. *Biophysical Journal.* 63:710–722.

Nir, S., T. Stegmann, and J. Wilschut. 1986. Fusion of influenza virus with cardiolipin liposomes at low pH: mass action analysis of kinetics and extent. *Biochemistry.* 25:257–266.

Puri, A., F. P. Booy, R. W. Doms, J. M. White, and R. Blumenthal. 1990. Conformational changes and fusion activity of influenza virus hemagglutinin of the H2 and H3 subtypes: effects of acid pretreatment. *Journal of Virology.* 64:3824–3832.

Sarkar, D. P., S. J. Morris, O. Eidelman, J. Zimmerberg, and R. Blumenthal. 1989. Initial stages of influenza hemagglutinin-induced cell fusion monitored simultaneously by two fluorescent events: cytoplasmic continuity and lipid mixing. *Journal of Cell Biology.* 109:113–122.

Siegel, D. P. 1993. Modeling protein-induced fusion mechanisms: insights from the relative stability of lipidic structures. *In* Viral Fusion Mechanisms. J. Bentz, editor. CRC Press, Boca Raton, FL. 475–512.

Skehel, J. J., P. M. Bayley, E. B. Brown, S. R. Martin, M. D. Waterfield, and J. M. White. 1982. Change in the conformation of influenza virus hemagglutinin at the pH optimum of virus-mediated membrane fusion. *Proceedings of the National Academy of Sciences.* 79:968–972.

Spruce, A. E., L. J. Breckenridge, A. K. Lee, and W. Almers. 1990. Properties of the fusion pore that forms during exocytosis of a mast cell secretory vesicle. *Neuron.* 4:643–654.

Spruce, A. E., A. Iwata, J. M. White, and W. Almers. 1989. Patch clamp studies of single cell-fusion events mediated by a viral fusion protein. *Nature.* 342:555–558.

Spruce, A. E., A. Iwata, and W. Almers. 1991. The first milliseconds of the pore formed by a fusogenic viral envelope protein during membrane fusion. *Proceedings of the National Academy of Sciences, USA.* 88:3623–3627.

Stegmann, T., F. P. Booy, and J. Wilschut. 1987a. Effect of low pH on influenza virus. Activation and inactivation of the membrane fusion capacity of the hemagglutinin. *Journal of Biological Chemistry.* 262:17744–17749.

Stegmann, T., J. M. Delfino, F. M. Richards, and A. Helenius. 1991. The HA2 subunit of influenza hemagglutinin inserts into the target membrane prior to fusion. *Journal of Biological Chemistry.* 266:18404–18410.

Stegmann, T., D. Hoekstra, G. Scherpof, and J. Wilschut. 1986. Fusion activity of influenza virus: A comparison between biological and artificial target membrane vesicles. *Journal of Biological Chemistry.* 261:10966–10969.

Stegmann, T., H. W. M. Morselt, F. P. Booy, J. F. L. van Breemen, G. Scherphof, and J. Wilschut. 1987b. Functional reconstitution of influenza virus envelopes. *EMBO Journal.* 6:2651–2659.

Stegmann, T., S. Nir, and J. Wilschut. 1989. Membrane fusion activity of influenza virus. Effects of gangliosides and negatively charged phospholipids in target liposomes. *Biochemistry.* 28:1698–1704.

Stegmann, T., J. M. White, and A. Helenius. 1990. Intermediates in influenza induced membrane fusion. *EMBO Journal.* 9:4231–4241.

Suzuki, Y., Y. Nagao, H. Kato, M. Matsumoto, K. Nerome, K. Nakajima, and E. Nobusawa. 1986. Human influenza A virus hemagglutinin distinguishes sialyloligosaccharides in membrane-associated gangliosides as its receptor which mediates the adsorption and fusion process of virus infection. *Journal of Biological Chemistry.* 261:17057–17061.

Tse, F. W., A. Iwata, and W. Almers. 1993. Membrane flux through the pore formed by a fusogenic viral envelope protein during cell fusion. *Journal of Cell Biology.* 121:543–552.

White, J. M. 1992. Membrane Fusion. *Science.* 258:917–924.

White, J. M., A. Helenius, and M.-J. Gething. 1982. Haemagglutinin of influenza virus expressed from a cloned gene promotes membrane fusion. *Nature.* 300:658–659.

White, J. M., M. Kielian, and A. Helenius. 1983. Membrane fusion proteins of enveloped viruses. *Quarterly Review of Biophysics.* 16:151–195.

Wiley, D. C., and J. I. Skehel. 1987. The structure and function of the hemagglutinin membrane glycoprotein of influenza virus. *Annual Review of Biochemistry.* 56:365–394.

Wunderli-Allenspach, H., and S. Ott. 1990. Kinetics of fusion and lipid transfer between virus receptor containing liposomes and influenza viruses as measured with the octadecylrhodamine B chloride assay. *Biochemistry.* 29:1990–1997.

Zimmerberg, J., R. Blumenthal, D. Sarkar, M. Curran, and S. J. Morris. 1993. Formation of multiple small pores and lipid flow in influenza HA-mediated membrane fusion. *Biophysical Journal.* 64:188a. (Abstr.)

Zimmerberg, J., M. Curran, and F. S. Cohen. 1991. A lipid/protein complex hypothesis for exocytotic fusion pore formation. *Annals of the New York Academy of Science.* 635:307–317.

Zimmerberg, J., M. Curran, F. S. Cohen, and M. Brodwick. 1987. Simultaneous electrical and optical measurements show that membrane fusion precedes secretory granule swelling during exocytosis of beige mouse mast cells. *Proceedings of the National Academy of Sciences, USA.* 84:1585–1589.